Geophysical Research Letters

RESEARCH LETTER
10.1029/2022GL101870

Artificial Upwelling—A Refined Narrative

M. Jürchott[1], A. Oschlies[1], and W. Koeve[1]

[1]GEOMAR Helmholtz Centre for Ocean Research Kiel, Kiel, Germany

Key Points:

- Artificial upwelling (AU) effectiveness to draw down CO_2 from the atmosphere is strongly dependent on the future CO_2 emission scenario
- The solubility pump becomes as effective as the biological carbon pump under high emission scenarios
- Organic matter transfer efficiency decreases under AU, likely due to higher water temperatures below the ocean's surface

Supporting Information:

Supporting Information may be found in the online version of this article.

Correspondence to:

M. Jürchott,
mjuerchott@geomar.de

Citation:

Jürchott, M., Oschlies, A., & Koeve, W. (2023). Artificial upwelling—A refined narrative. *Geophysical Research Letters*, *50*, e2022GL101870. https://doi.org/10.1029/2022GL101870

Received 25 OCT 2022
Accepted 31 JAN 2023

Author Contributions:

Conceptualization: M. Jürchott, W. Koeve
Data curation: M. Jürchott, W. Koeve
Formal analysis: M. Jürchott
Investigation: M. Jürchott
Methodology: W. Koeve
Supervision: A. Oschlies, W. Koeve
Validation: W. Koeve
Visualization: M. Jürchott
Writing – original draft: M. Jürchott
Writing – review & editing: M. Jürchott, A. Oschlies, W. Koeve

Abstract The current narrative of artificial upwelling (AU) is to translocate nutrient rich deep water to the ocean surface, thereby stimulating the biological carbon pump (BCP). Our refined narrative takes the response of the solubility pump and the CO_2 emission scenario into account. Using global ocean-atmosphere model experiments we show that the effectiveness of a hypothetical maximum AU deployment in all ocean areas where AU is predicted to lower surface pCO_2, the draw down of CO_2 from the atmosphere during years 2020–2100 depends strongly on the CO_2 emission scenario and ranges from 1.01 Pg C/year (3.70 Pg CO_2/year) under RCP 8.5 to 0.32 Pg C/year (1.17 Pg CO_2/year) under RCP 2.6. The solubility pump becomes equally effective compared to the BCP under the highest emission scenario (RCP 8.5), but responds with CO_2 outgassing under low CO_2 emission scenarios.

Plain Language Summary Artificial upwelling (AU) is a proposed marine carbon dioxide removal (CDR) method, which suggests deploying pipes in the ocean to pump deep water to the ocean's surface. This process theoretically has several different impacts on the surface layer including an increase in the nutrient concentration, as well as a decrease in surface water temperature. Changes in the carbon cycle and associated with biological components are covered by the biological carbon pump (BCP), while changes via physical-chemical processes are covered by the solubility pump. Using numerical ocean modeling and simulating almost globally applied AU between the years 2020 and 2100 under several different atmospheric CO_2 emission scenarios, we show that AU leads under every simulated emission scenario to an additional CO_2-uptake of the ocean, but the potential increases under higher emission scenarios (up to 1.01 Pg C/year (3.70 Pg CO_2/year) under the high CO_2-emission scenario RCP 8.5). The individual contribution via the BCP is under every emission scenario positive, while the processes associated with the solubility pump can lead to CO_2-uptake under higher emission scenarios and CO_2 outgassing under lower emission scenarios.

1. Introduction

Earths' atmospheric CO_2 concentration (pCO_2^{atm}) has strongly increased since preindustrial times and continues to rise despite considerable CO_2 emission reduction efforts (IPCC, 2022). Assuming that humanity ambitiously intensifies emission reduction efforts, we still have to deal with hard-to-abate CO_2 emissions (Thoni et al., 2020). To compensate these residual emissions and reach a net zero carbon emission world around mid century, we likely need to actively remove CO_2 from the atmosphere (IPCC, 2022), which has led to an increased interest in marine carbon dioxide removal (CDR) technologies (GESAMP, 2019).

One proposed marine CDR idea is to use artificial upwelling (AU) to pump up nutrients from the interior ocean to the sea surface via ocean pipes to stimulate the biological carbon pump (BCP) (Lovelock & Rapley, 2007). This process is supposed to enhance primary production (PP) at the sea surface, thereby increase export production (EP) and finally lead to a net CO_2 flux from the atmosphere into the interior ocean. Several studies have already shown that this simplistic view of stimulating the BCP (Volk & Hoffert, 1985) via AU is not sufficient for a comprehensive evaluation of this technology in terms of its carbon drawdown potential and its climate effects (Dutreuil et al., 2009; Keller et al., 2014; Oschlies et al., 2010; Yool et al., 2009). Especially pumping up water with a high concentration of dissolved inorganic carbon (DIC) may even lead to a net CO_2 outgassing despite an increase in EP (Dutreuil et al., 2009). Nevertheless, the prevailing narrative of viewing AU and it's CDR potential as being primary driven by the BCP, and therefore independent of the underlying CO_2-emission scenario, still remains (Baumann et al., 2021; GESAMP, 2019; Koweek, 2022).

One may be tempted to argue that AU in a fixed C-N-P stoichiometry ("Redfield") world model should result in a net zero carbon uptake through the BCP. However, pumping up preformed nutrients (Duteil et al., 2012) to the sea surface may contribute to an additional carbon uptake. AU will also affect properties such as alkalinity, sea

surface temperature and preformed DIC, which collectively may cause a response of the solubility pump (Volk & Hoffert, 1985) with the potential to influence the atmosphere to ocean carbon flux, too. Also the dependence of the CO_2-uptake due to AU on the atmospheric pCO_2 path (the assumption of the underlying CO_2 emission scenario) under which it takes place is not well understood.

To get a better understanding of the effects of AU and the processes involved, we simulate AU in an Earth System model of intermediate complexity combined with an idealized tracer approach and under a range of CO_2 emission scenarios to (a) evaluate the general impact of AU on the ocean's carbon uptake under different CO_2 emission scenarios, (b) to explicitly quantify the respective importance of the BCP and the solubility pump in the model simulations, and (c) to identify the important carbon uptake, release and storage regions in the ocean.

2. Methods

2.1. Model

We use the UVic 2.9 Earth System model of intermediate complexity (Keller et al., 2012; Weaver et al., 2001) in a noLand configuration with a dynamically coupled atmosphere, sea-ice and ocean component (Gent & Mcwilliams, 1990; Koeve et al., 2020; Orr et al., 1999). A detailed description of this model version is given in the Methods section in Supporting Information S1. The three-dimensional ocean component has a spatial resolution of 3.6° longitude and 1.8° latitude and consists of 19 vertical levels with 50 m thickness close to the surface and up to 500 m in the deep ocean. The used model version contains a fully simulated carbon cycle including DIC and alkalinity as prognostic tracers, a marine ecosystem model representation of the BCP in which we assume a fixed C-N-P organic matter stoichiometry (Keller et al., 2012), as well as a simple $CaCO_3$ counter pump approximation (Schmittner et al., 2008). In the model PP is not sensitive to CO_2 and the nutrients nitrate and phosphate are simulated as prognostic tracers, while iron-limitation is prescribed via an iron concentration mask at the oceans surface layer (Galbraith et al., 2010).

In our UVic 2.9 noLand model version all interactions with the land-component are disabled in order to isolate the effects of AU exclusively on the ocean. The use of a noLand model allows us to better understand and distinguish the involved processes and effects of AU especially on the marine carbon cycle.

2.2. Simulating AU

The simulation of AU is adopted from previous studies conducted with an earlier version of the UVic model (Keller et al., 2014; Oschlies et al., 2010). Model tracers like nutrients, temperature, DIC and alike are transferred via AU adiabatically from the lowest grid box at the end of the pipes to the surface grid box at a rate of 1 cm/day averaged over the area of the grid box, while a compensating down-welling flux through all intermediate levels ensures volume conservation. AU-induced changes in for example, the temperature depth profile change water column physics, circulation and impact the simulated ecosystem. To replace 1 cm/day of surface water it would be necessary to deploy a dense network of pipes, for example, with one pipe per square kilometer, each with a volumetric flow rate of about 0.12 m^3/s (Koweek, 2022). A deployment algorithm is used at model runtime to automatically deploy the ocean pipes only where (a) the phosphate concentration is lower than a threshold concentration at the sea surface (0.4 $mmol/m^3$ in this study) and (b) complete uptake of upwelled macronutrients would lead to a reduction in local surface-water pCO_2 (Figure 1c, Figures S1 and S2a in Supporting Information S1). This procedure ensures that pipes are only deployed in regions where CO_2 outgassing is unlikely. It turns out that almost all regions where pipes meet these conditions for deployment at any time during the simulation, subsequently maintain these conditions throughout the simulations. Additionally, the length of the pipes is limited to 1000 m and optimized by the algorithm to maximize for additional local CO_2-uptake (Figure S2b in Supporting Information S1). Besides upwelling nutrients, AU has an impact on all other tracers including DIC, alkalinity, salinity and temperature. Since our model does not include a dynamic iron cycle, we follow the approach of Keller et al. (2014) and assume that AU relaxes any iron limitation at the sea surface in regions where pipes are deployed. Hence, our experiments considered a best-case scenario for the impact of a close to global application of AU on a Redfield-like BCP.

2.3. Separation of Marine Carbon Pumps

The separation of the marine carbon pumps is achieved by introducing two idealized tracers to the model, which measure the individual impact on the carbon cycle via the BCP (DIC^{rem}) and the solubility pump (DIC^{pre})

Table 1
Model Experiments Conducted With the UVic 2.9 ESM NoLand Model Version

Name	Emission forcing	Pipe simulation
REF_0.0	no-emission	No pipes
REF_2.6	RCP 2.6	No pipes
REF_4.5	RCP 4.5	No pipes
REF_6.0	RCP 6.0	No pipes
REF_8.5	RCP 8.5	No pipes
ArtUp_0.0	no-emission	Pipes
ArtUp_2.6	RCP 2.6	Pipes
ArtUp_4.5	RCP 4.5	Pipes
ArtUp_6.0	RCP 6.0	Pipes
ArtUp_8.5	RCP 8.5	Pipes

(Bernardello et al., 2014; Koeve et al., 2020). The idealized tracer DIC^{rem} is set to zero upon any contact with the atmosphere and increases in the interior ocean by the amount of DIC released into the water column via organic matter degradation, thus exclusively counting the amount of DIC tracing back to the BCP. The idealized tracer DIC^{pre} adopts the value of total DIC at the surface layer and preserves it while being transported to greater depth through ocean circulation. Therefore, DIC^{pre} exclusively counts the amount of DIC added to the interior ocean via physical-chemical processes at the ocean's surface that are associated with the solubility pump. There is no explicit idealized tracer of DIC stored in the interior ocean by means of the $CaCO_3$ counter pump. DIC^{ca}, however, may be diagnosed from $DIC^{ca} = DIC - DIC^{pre} - DIC^{rem}$. As discussed below, any change in DIC^{ca} should not be confused with the impact of a changing $CaCO_3$ counter pump on atmospheric pCO_2. The idealized tracer Ideal-Age (calculated similar compared to DIC^{rem}) counts the time of a water mass since it was last in contact with the atmosphere and therefore, provides additional information about the age of a water mass in the interior ocean (England, 1995; Koeve & Kähler, 2016). All three idealized tracers are influenced by ocean circulation and mixing, but do not interact with other model tracers.

2.4. Experimental Design

Following model spin-up under preindustrial conditions we simulate the historical period from the year 1765 to 2006 with CO_2-emissions to the atmosphere, which are consistent with historical fossil fuel and land-use carbon emissions and apply from 2006 to 2100 different CO_2-emission forcings consistent with RCP 2.6, 4.5, 6.0 and 8.5 (Meinshausen et al., 2011), which are corrected for the noLand model configuration (Table 1, Figure S3 and Methods in Supporting Information S1) (Koeve et al., 2020). This makes sure that the noLand reference model experiments (REF) experience the same climate change as do fully coupled (with Land) counterparts. An idealized no-emission model simulation applies AU in a hypothetical world without any historical or future CO_2 emissions. We simulated the effects of AU in the ArtUp-simulations for the time period 2020 to 2100 and performed respective reference simulations (REF) without AU for comparisons. By comparing the ArtUp- to the Reference-simulation (i.e., ArtUp–REF) conducted under the same CO_2 emission scenario we can explicitly study the effects of applied AU. We compared these results with respect to the different CO_2 emission scenarios to study the effectiveness of AU under different CO_2 emission scenarios.

3. Results

3.1. Impact of AU on the Ocean's Carbon Budget

AU leads to a carbon drawdown from the atmosphere into the ocean in comparison to the respective REF simulation, while the additional ocean's carbon uptake is strongly dependent on the RCP CO_2 emission scenario over the course of the experiments (Figures 1b and 1d). Under the RCP 8.5 and RCP 6.0 CO_2 emission scenarios, AU leads to an almost linear and continuous carbon drawdown from the atmosphere into the ocean (on average 1.01 Pg C/year for RCP 8.5; multiply by 3.664 for conversion to Pg CO_2), while the carbon drawdown under the RCP 4.5 CO_2 emission scenario starts to slow down after 50 years of pipe deployment. Under the RCP 4.5 CO_2 emission scenario the cumulative carbon drawdown after 80 years is already ∼50% less compared to the RCP 8.5 CO_2 emission scenario simulation. The RCP 2.6 CO_2 emission scenario and the no-emission simulation show an even earlier and stronger decline in the ocean's AU-induced carbon uptake, until they reach a plateau after a few decades (on average 0.32 Pg C/year for RCP 2.6). The model simulations show that the potential of AU to draw down carbon from the atmosphere increases with higher CO_2 emission scenarios, while the carbon drawdown potential decreases and even stagnates under lower CO_2 emission scenarios.

3.2. Biological Carbon Pump Versus Solubility Pump

In the global deployment scenario, the BCP responds to AU under every CO_2 emission scenario by an additional carbon uptake and only shows a moderate emission scenario dependency, while the solubility pump shows a strong

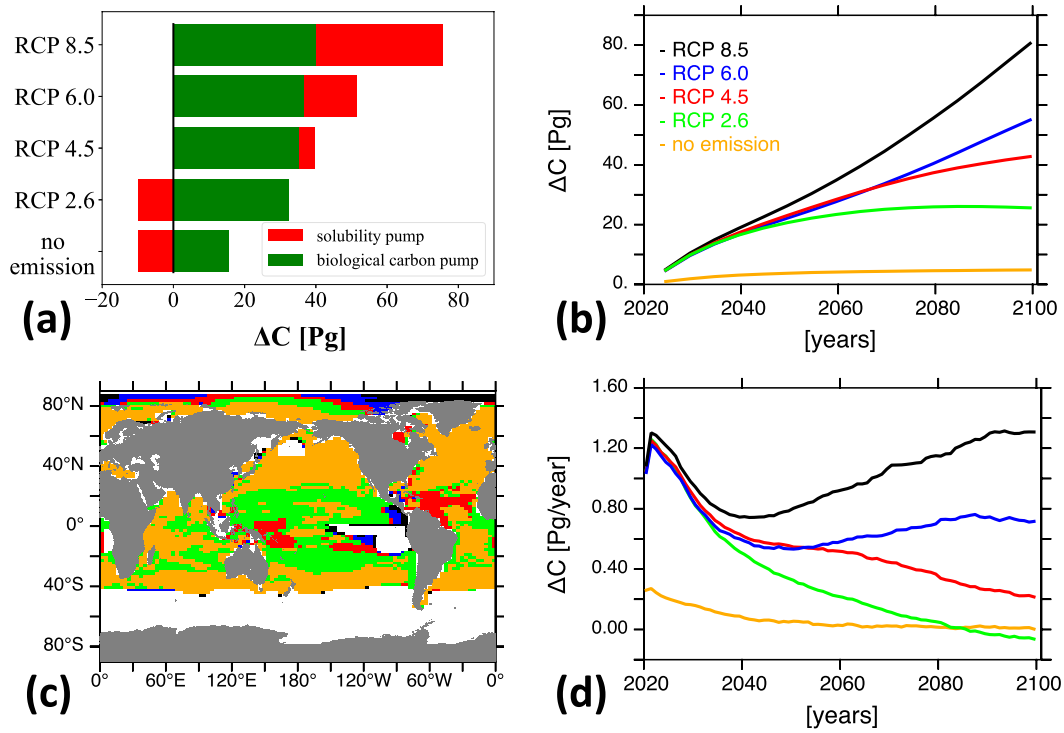

Figure 1. Pipe covered area and global carbon uptake from artificial upwelling (AU). (a) Cumulative net increase in the ocean's carbon budget in the year 2100 (Pg C) due to AU, divided into the individual carbon uptake of the biological carbon pump (green) and the solubility pump (red). Time history of (b) cumulative and (d) annual average net increase in the ocean's carbon budget via AU compared to respective reference simulation for different CO_2 emission scenarios (ArtUp–REF; Pg C, see Figure S4 in Supporting Information S1 as well). (c) Pipe covered area in year 2100 (plotted pipe covered area of each emission scenarios includes the area of lower CO_2 emission scenarios); color code as indicated in (b); see Figures S1 and S2a in Supporting Information S1 for details.

emission scenario dependency and can even release carbon into the atmosphere and thereby counter the BCP uptake under low emission scenarios (Figure 1a). Since we apply a fixed C-N-P stoichiometry for PP and degradation in our model, the additional carbon uptake via the BCP cannot be explained by pumping up re-mineralized nutrients, but by introducing preformed nutrients from the interior ocean to the sea surface (Figure 2a). Preformed nutrients are nutrients, which leave the surface ocean by circulation, particularly in temperate and high latitude

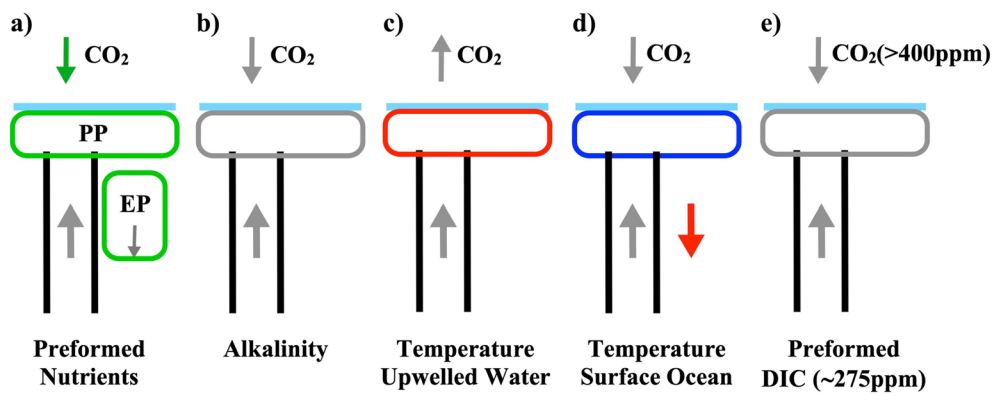

Figure 2. Theoretical concept of the processes stimulated by artificial upwelling (black lines) and their impact on the air-sea CO_2 flux and the surface ocean (box below air-sea boundary). Arrows in the atmosphere indicate air-sea CO_2 flux direction, arrows in the ocean indicate tracer movement and colors red/blue indicate respective water temperature increase/decrease. (a) Covers the increase in primary production and export production associated with the biological carbon pump (green), (b)–(e) cover the impacts of the individual processes associated with the solubility pump.

regions, without being taken up by primary producers for example, due to iron or light limitation and do not come with a Redfield-equivalent CO_2 counterpart (Figure S5 in Supporting Information S1). Thus, preformed nutrients can lead to an additional carbon uptake via the BCP. The fixed stoichiometry also implies that pumping up DIC^{rem} to the sea surface will not lead to an outgassing of CO_2 into the atmosphere as long as its re-mineralized nutrient counterpart gets taken up close to the pipes by primary producers again.

The response of the solubility pump can be explained by a combination of several processes including pumping up alkalinity, preformed DIC and changes in water temperature. In the global average, the alkalinity concentration in our model increases with depth due to $CaCO_3$ production at the sea surface and dissolution in the interior ocean (Figure S6a in Supporting Information S1). By simulating AU we pump up alkalinity, on average, which translates into alkalinity enhancement at the sea surface similar to what is intended by artificial ocean alkalinity enhancement by adding minerals like olivine to the ocean surface (Hartmann et al., 2013; Köhler et al., 2010). Ocean alkalinity enhancement is associated with a CO_2 flux from the atmosphere into the ocean (Figure 2b) (Keller et al., 2014), but since the amount of alkalinity added to the sea surface is about the same under every emission scenario in our experiments (Figure S6b in Supporting Information S1), we do expect a similar CO_2-uptake effect and therefore, this process can most likely not explain the dependency of the solubility pump to the emission scenario. AU also results in a change in water temperatures, since the water pumped up from the deep ocean is significantly colder compared to the surface water. At the surface, the pumped up water increases in temperature (decrease in max. CO_2-solubility; Figure 2c), while it is cooling down the surface ocean at the same time (increase in max. CO_2-solubility; Figure 2d). Both carbon fluxes related to temperature effects will partly counteract each other, but since, over the area where pipes are deployed, the relative temperature increase of the pumped up water is much greater than the relative temperature decrease of the surface water (Figure S7 in Supporting Information S1), the net effect on the carbon flux is expected to result in CO_2 outgassing into the atmosphere. Furthermore, AU pumps up DIC^{pre} from the interior ocean to the sea surface and in contact with the atmosphere (Figure 2e). DIC^{pre} is the amount of carbon taken up by the ocean via physical-chemical processes and its concentration in the interior ocean strongly depends on the pCO_2^{atm} concentration and water temperature at the time and location of the water mass formation region. The water pumped up is mostly old enough to be equilibrated under preindustrial pCO_2^{atm} levels (~275 ppm; Figure 3c) and bringing it in contact with an elevated pCO_2^{atm} level (>400 ppm, except for the no-emission scenario) results in a carbon flux from the atmosphere into the ocean, which also increases under higher emission scenarios (Figure S8 in Supporting Information S1). While a quantitative separation of the individual processes influencing the response of the solubility pump is challenging (and beyond the scope of this paper), we propose from the discussion above that the outgassing under the RCP 2.6 emission scenario is most likely dominated by the temperature increase of the pumped-up water. Under higher emission scenarios the positive impact of pumping up water to the sea surface, which had been equilibrated under preindustrial atmospheric CO_2 levels exceeds the negative impact of the temperature increase of the pumped up water mass.

3.3. Carbon Storage Depths and Location

For the RCP 8.5 emission scenario 56.1 Pg C (69.5%) of the AU-induced air-sea carbon flux gets added below the maximum pipes source depths of 1200 m and can be referred to as stored over the next centuries (Table S1 in Supporting Information S1) (Lampitt et al., 2008; Siegel et al., 2021). Using pump-specific tracers, we diagnose individual shares of 11.6 Pg C (20.7%) for the BCP and 22.6 Pg C (40.2%) for the solubility pump. The remaining 21.9 Pg C (39.1%), computed as residual (see Section 2), is assumed to be associated with the carbon export via the $CaCO_3$ counter pump (but see discussion below). Therefore, 63.5% of the total carbon taken up via the solubility pump and only 29% of the total carbon taken up via the BCP gets stored below 1200 m. The inefficiency of the BCP to add carbon below 1200 m gets amplified through AU by a reduction in the global transfer efficiency (T_{eff}) of −7.2% (Table S2 in Supporting Information S1). The transfer efficiency, here calculated as the integral of remineralized detritus ≥1200 m/remineralized detritus ≥130 m, gives an estimate of how strong the organic matter degradation is between the carbon export depth and the carbon storage depth. A reduction in T_{eff} triggered by AU indicates a higher organic matter degradation rate between 130 and 1200 m (reasons discussed below). Overall, the budget changes of DIC, DIC^{pre}, and DIC^{rem} show that a substantial amount of the carbon added to the ocean via AU gets stored below the maximum source depths of the pipes, with the solubility pump showing a high efficiency in transporting the additional carbon to the deep ocean.

The increased carbon uptake of the ocean via AU below 1200 m is unevenly distributed in the ocean with hotspots in the North Atlantic, North Pacific and around the equator (Figure 3b). The solubility pump is the main driver

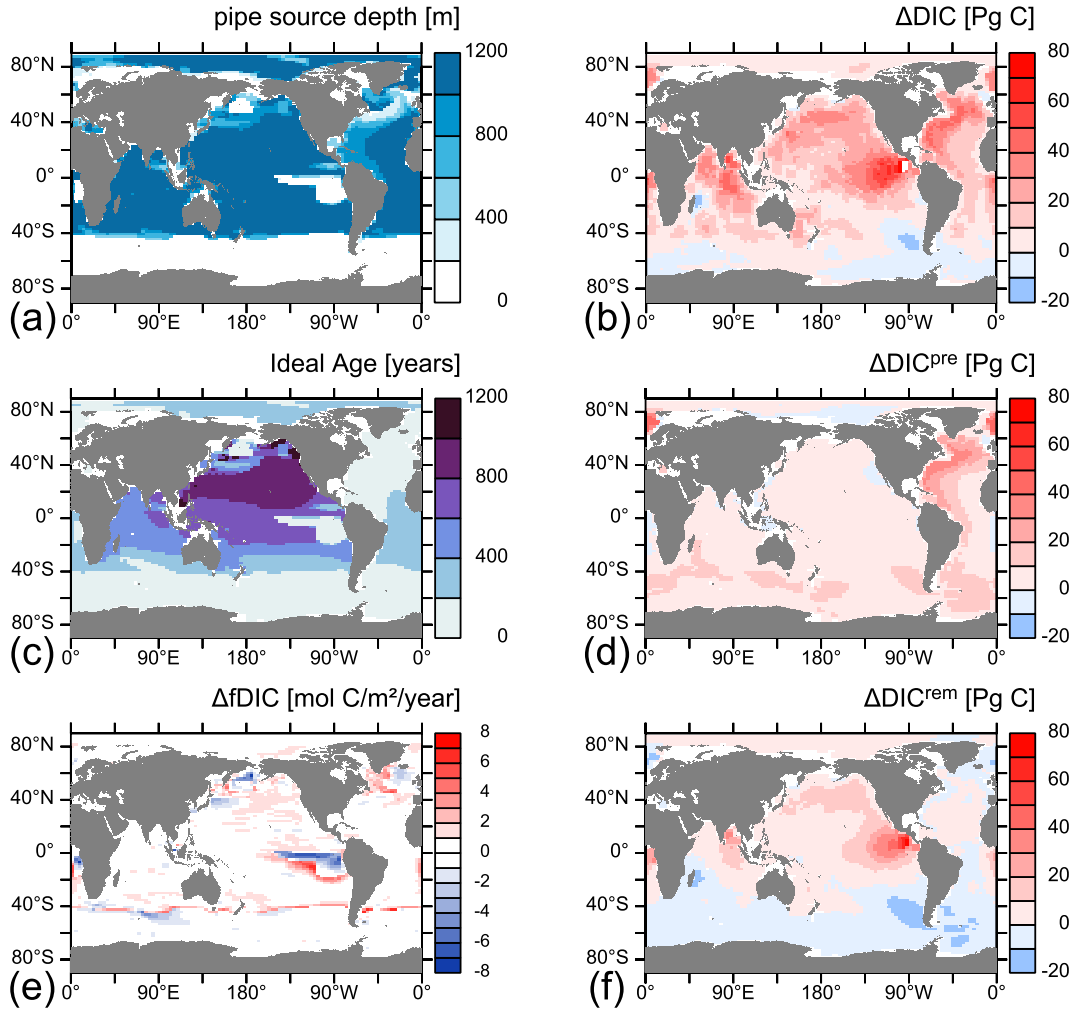

Figure 3. Regional effects of artificial upwelling for experiments under the RCP 8.5 emission scenarios for the year 2100. (a) Pipe distribution and pipe source depth (m). (c) Average age (since last contact with the atmosphere) of water at pipes source depth (years). (e) CO_2 flux at ocean-atmosphere boundary (positive downward; mol C m^{-2} $year^{-1}$). (b, d, f) Cumulative net change in dissolved inorganic carbon (DIC) (b), DIC^{pre} (d) and DIC^{rem} (f) below 1200m depths from 2020 to 2100 compared to the respective reference simulation (ArtUp–REF; Pg C).

for the additional carbon storage in the North Atlantic (Figure 3d). The additional carbon uptake of the solubility pump has its origin at the atmosphere to ocean boundary (Figure 3e) and the shallow pipes in the north Atlantic (Figure 3a) cannot explain the carbon transport below the pipes source depth. Thus, we propose that one contributing factor to the high efficiency of the solubility pump in this region is the large-scale ocean circulation. The CO_2-uptake via the BCP below 1200 m related to AU is dominated by the central-east Pacific region (Figure 3f). This region has a strong naturally occurring stratification, which gets first undermined by the pipe's pumping action and second weakened by the temperature exchange between the surface water and the deep ocean. Thus, the temperature gradient between the surface water and the deep ocean decreases and allows preformed nutrients to enter the surface ocean more efficiently. This results in an additional carbon uptake via an enhanced BCP and leads to a greater export of DIC^{rem} below 1200 m.

4. Discussion

The residual portion of 21.9 Pg C below 1,200 m that is attributed neither to the BCP nor to the solubility pump, is associated with the $CaCO_3$ counter pump. This additional deep carbon flux leaves the impression of the $CaCO_3$ counter pump being important in terms of additional ocean CO_2-uptake, but, as is well known, the $CaCO_3$

counter pump cannot constitute a CO_2 flux into the ocean due to its flux of alkalinity being twice as high as the DIC flux (Riebesell et al., 2009). In our model, the production of $CaCO_3$ is linked to the detritus production of the ecosystem model (see Methods in Supporting Information S1) and thus, gets indirectly stimulated via any increase in PP. However, more intensive $CaCO_3$ export from the surface ocean would reduce the surface ocean CO_2-buffer capacity and reduce CO_2-uptake via the solubility pump. Due to the non-linearity of the CO_2 system it is not straightforward to quantify how the apparent storage (i.e., increase in DIC^{ca}, Figure S9 in Supporting Information S1) associated with this increase of the $CaCO_3$ counter pump translates into a CO_2-flux between ocean and atmosphere.

Concerning the reduction of the transfer efficiency under AU, we propose that this might be a result of an increase in water temperature below the cooled surface layer (Figure S10 in Supporting Information S1). Organic matter degradation speeds up under higher water temperatures, which results in shallower degradation depth. AU and the compensating downward flow result in a net downward heat flux to greater depth. This side effect of AU was discovered and discussed in previous papers and causes, after AU termination, a strong increase in surface air temperature and pCO_2^{atm} levels beyond the reference simulations (Keller et al., 2014; Oschlies et al., 2010). Here we report that the AU-induced heat transport to greater depth also has a negative impact on the organic matter transfer efficiency during AU deployment.

Discussing the limits of our study, the used noLand model configuration does not allow for feedbacks of ocean-atmosphere interactions on the land component and vice versa. In our idealized model study, surface ocean and atmospheric cooling via AU hence does not increase the carbon uptake on land as reported in previous studies (Keller et al., 2014; Oschlies et al., 2010), nor does this land CO_2-uptake potentially affect the marine CO_2-uptake. Therefore, the earth's net carbon uptake via AU presented in our study might be higher, if the land biosphere component is included. Changes in our experimental protocol in how AU is simulated (e.g., pipe covered area, pipe length, upwelled volume, duration period, iron limitation) might change the ocean's net carbon uptake and the individual contributions via the solubility pump and the BCP as well (Koweek, 2022; Oschlies et al., 2010; Yool et al., 2009).

5. Conclusion and Outlook

Our results indicate that only addressing processes associated with the BCP does not accurately reflect the CDR potential of AU. The additional carbon uptake of the ocean is strongly dependent on the CO_2 emission scenario. The BCP is able to take up additional carbon in the assumed global AU deployment under every emission scenario, but shows a low efficiency in exporting DIC^{rem} below the maximum pipe source depth of 1200 m except for the central-east Pacific region. This suggests that most of the CO_2-uptake stimulated by AU and attributable to an increase of the BCP will potentially be rather short lived. The main driver for the AU-enhanced BCP is the decreased stratification and the increased access of primary producers to preformed nutrients, while the decrease in the transfer efficiency might be a side effect of faster organic matter degradation due to higher water temperatures below the sea surface.

The solubility pump shows a strong CO_2 emission scenario dependency and can lead to CO_2 outgassing under low emission scenarios, which can almost completely mitigate the additional CO_2-uptake via the BCP. Under high emission scenarios, the solubility pump can also take up equal amounts of additional CO_2 compared to the BCP. The solubility pump shows a high efficiency in exporting DIC^{pre} below the maximum pipes source depth and the large-scale ocean circulation in the North Atlantic including deep-water formation seems to play a key role in this regard.

Additional studies including new model experiments might be able to quantify the single processes associated with the solubility pump and to further investigate the high efficiency CO_2 export regions identified in this study. Going beyond the Redfield world and assuming higher C-N ratios in organic matter produced via AU as proposed recently from experimental work (Baumann et al., 2021), as well as simulating the potentially limited supply of iron (Tagliabue et al., 2017) in pipe-covered areas could further impact projections of the quantitative potential of the BCP in this CDR technique.

Data Availability Statement

Model output and scripts for data processing are available from data.geomar.de (https://hdl.handle.net/20.500.12085/9e4c269c-8fa3-4bb9-994f-e8c7a5cdefbb).

Acknowledgments
We acknowledge discussions with colleagues from the Biogeochemical Modelling research unit at GEOMAR. M.J. acknowledges funding from German BMBF, Project Test-ArtUp (Grant 03F0897A). This is a contribution to the CDRmare research mission funded by the German Alliance for Marine Research (DAM). The author(s) wish to acknowledge use of the PyFerret program for analysis and graphics in this paper. PyFerret is a product of NOAA's Pacific Marine Environmental Laboratory (Information is available at http://ferret.pmel.noaa.gov/Ferret/). Open Access funding enabled and organized by Projekt DEAL.

References

Baumann, M., Taucher, J., Paul, A. J., Heinemann, M., Vanharanta, M., Bach, L. T., et al. (2021). Effect of intensity and mode of artificial upwelling on particle flux and carbon export. *Frontiers in Marine Science*, *8*, 1579. https://doi.org/10.3389/fmars.2021.742142

Bernardello, R., Marinov, I., Palter, J. B., Galbraith, E. D., & Sarmiento, J. L. (2014). Impact of Weddell Sea deep convection on natural and anthropogenic carbon in a climate model. *Geophysical Research Letters*, *41*(20), 7262–7269. https://doi.org/10.1002/2014GRL061313

Duteil, O., Koeve, W., Oschlies, A., Aumont, O., Bianchi, D., Bopp, L., et al. (2012). Preformed and regenerated phosphate in ocean general circulation models: Can right total concentrations be wrong? *Biogeosciences*, *9*(5), 1797–1807. https://doi.org/10.5194/bg-9-1797-2012

Dutreuil, S., Bopp, L., & Tagliabue, A. (2009). Impact of enhanced vertical mixing on marine biogeochemistry: Lessons for geo-engineering and natural variability. *Biogeosciences*, *6*(5), 901–912. https://doi.org/10.5194/bg-6-901-2009

England, M. H. (1995). The age of water and ventilation timescales in a global ocean model. *Journal of Physical Oceanography*, *25*(11), 2756–2777. https://doi.org/10.1175/1520-0485(1995)025<2756:TAOWAV>2.0.CO;2

Galbraith, E. D., Gnanadesikan, A., Dunne, J. P., & His-cock, M. R. (2010). Regional impacts of iron-light colimitation in a global biogeochemical model. *Biogeosciences*, *7*(3), 1043–1064. https://doi.org/10.5194/bg-7-1043-2010

Gent, P. R., & Mcwilliams, J. C. (1990). Isopycnal mixing in ocean circulation models. *Journal of Physical Oceanography*, *20*(1), 150–155. https://doi.org/10.1175/1520-0485(1990)020<0150:IMIOCM>2.0.CO;2

GESAMP. (2019). High level review of a wide range of proposed marine geoengineering techniques. In P. W. Boyd & C. M. G. Vivian (Eds.), *Rep. Stud. GESAMP No. 98, (IMO/FAO/UNESCO-IOC/UNIDO/WMO/IAEA/UN/UN Environment/UNDP/ISA Joint Group of Experts on the Scientific Aspect of Marine Environmental Protection)* (p. 144). International Maritime Organisation.

Hartmann, J., West, A. J., Renforth, P., Köhler, P., De La Rocha, C. L., Wolf-Gladrow, D., et al. (2013). Enhanced chemical weathering as a geoengineering strategy to reduce atmospheric carbon dioxide, supply nutrients, and mitigate ocean acidification. *Reviews of Geophysics*, *51*(2), 113–149. https://doi.org/10.1002/rog.20004

IPCC. (2022). Summary for policymakers. In P. R. Shukla, J. Skea, R. Slade, A. Al Khourdajie, R. van Diemen, et al. (Eds.), *Climate change 2022: Mitigation of climate change. Contribution of working group III to the sixth assessment report of the intergovernmental panel on climate change*. Cambridge University Press. https://doi.org/10.1017/9781009157926.001

Keller, D. P., Feng, E. Y., & Oschlies, A. (2014). Potential climate engineering effectiveness and side effects during a high carbon dioxide-emission scenario. *Nature Communications*, *5*(1), 1–11. https://doi.org/10.1038/ncomms4304

Keller, D. P., Oschlies, A., & Eby, M. (2012). A new marine ecosystem model for the University of Victoria Earth System Climate Model. *Geoscientific Model Development*, *5*(5), 1195–1220. https://doi.org/10.5194/gmd-5-1195-2012

Koeve, W., & Kähler, P. (2016). Oxygen utilization rate (OUR) underestimates ocean respiration: A model study. *Global Biogeochemical Cycles*, *30*(8), 1166–1182. https://doi.org/10.1002/2015GB005354

Koeve, W., Kähler, P., & Oschlies, A. (2020). Does export production measure transient changes of the biological carbon pump's feedback to the atmosphere under global warming? *Geophysical Research Letters*, *47*(22), e2020GL089928. https://doi.org/10.1029/2020GL089928

Köhler, P., Hartmann, J., & Wolf-Gladrow, D. A. (2010). Geoengineering potential of artificially enhanced silicate weathering of olivine. *Proceedings of the National Academy of Sciences*, *107*(47), 20228–20233. https://doi.org/10.1073/pnas.1000545107

Koweek, D. A. (2022). Expected limits on the potential for carbon dioxide removal from artificial upwelling. *Frontiers in Marine Science*, *9*, 841894. https://doi.org/10.3389/fmars.2022.841894

Lampitt, R. S., Achterberg, E. P., Anderson, T. R., Hughes, J. A., Iglesias-Rodriguez, M. D., Kelly-Gerreyn, B. A., et al. (2008). Ocean fertilization: A potential means of geoengineering? *Philosophical Transactions of the Royal Society A: Mathematical, Physical & Engineering Sciences*, *366*(1882), 3919–3945. https://doi.org/10.1098/rsta.2008.0139

Lovelock, J. E., & Rapley, C. G. (2007). Ocean pipes could help the Earth to cure itself. *Nature*, *449*(7161), 403. https://doi.org/10.1038/449403a

Meinshausen, M., Smith, S. J., Calvin, K. V., Daniel, J. S., Kainuma, M. L. T., Lamarque, J.-F., et al. (2011). The RCP greenhouse gas concentrations and their extension from 1765 to 2300. *Climatic Change*, *109*(1–2), 213–241. https://doi.org/10.1007/s10584-011-0156-z

Orr, J. C., Najjar, R., Sabine, C. L., & Joos, F. (1999). Abiotic-HOWTO, internal OCMIP report, LSCE/CEA Saclay, Gif-sur-Yvette, France (p. 25).

Oschlies, A., Pahlow, M., Yool, A., & Matear, R. J. (2010). Climate engineering by artificial ocean upwelling: Channelling the sorcerer's apprentice. *Geophysical Research Letters*, *37*(4), L04701. https://doi.org/10.1029/2009GL041961

Riebesell, U., Körtzinger, A., & Oschlies, A. (2009). Sensitivities of marine carbon fluxes to ocean change. *Proceedings of the National Academy of Sciences*, *106*(49), 20602–20609. https://doi.org/10.1073/pnas.0813291106

Schmittner, A., Oschlies, A., Matthews, H. D., & Galbraith, E. D. (2008). Future changes in climate, ocean circulation, ecosystems, and biogeochemical cycling simulated for a business-as-usual CO_2 emission scenario until year 4000 AD. *Global Biogeochemical Cycles*, *22*(1), GB1013. https://doi.org/10.1029/2007GB002953

Siegel, D. A., DeVries, T., Doney, S. C., & Bell, T. (2021). Assessing the sequestration time scales of some ocean-based carbon dioxide reduction strategies. *Environmental Research Letters*, *16*(10), 104003. https://doi.org/10.1088/1748-9326/ac0be0

Tagliabue, A., Bowie, A. R., Boyd, P. W., Buck, K. N., Johnson, K. S., & Saito, M. A. (2017). The integral role of iron in ocean biogeochemistry. *Nature*, *543*(7643), 51–59. https://doi.org/10.1038/nature21058

Thoni, T., Beck, S., Borchers, M., Förster, J., Görl, K., Hahn, A., et al. (2020). Deployment of negative emissions technologies at the national level: A need for holistic feasibility assessments. *Frontiers in Climate*, *2*, 590305. https://doi.org/10.3389/fclim.2020.590305

Volk, T., & Hoffert, M. I. (1985). Ocean carbon pumps: Analysis of relative strengths and efficiencies in ocean-driven atmospheric CO_2 changes. In *The carbon cycle and atmospheric CO_2: natural variations Archean to present* (Vol. 32, pp. 99–110). https://doi.org/10.1029/GM032p0099

Weaver, A. J., Eby, M., Wiebe, E. C., Bitz, C. M., Duffy, P. B., Ewen, T. L., et al. (2001). The UVic Earth System Climate Model: Model description, climatology, and applications to past, present and future climates. *Atmosphere-Ocean*, *39*(4), 361–428. https://doi.org/10.1080/07055900.2001.9649686

Yool, A., Shepherd, J. G., Bryden, H. L., & Oschlies, A. (2009). Low efficiency of nutrient translocation for enhancing oceanic uptake of carbon dioxide. *Journal of Geophysical Research*, *114*(C8), C08009. https://doi.org/10.1029/2008JC004792